Cholesterol Mesogen Containing Water-Soluble Copolymers: Design and Organization Behavior at Different Interfaces

K. Chandrasekar and Geetha Baskar*

Industrial Chemistry Laboratory, Central Leather Research Institute, Adyar, Chennai 600 020, India

Received December 30, 2006; Revised Manuscript Received February 19, 2007

Cholesterol mesogen containing monomer, cholesteryl acrylamido butyrate (CAB) with the novel spacer group drawn from 4-amino butyric acid has been demonstrated to exhibit good reactivity with 2-acrylamido-2-methyl-1-propane sulfonic acid (AMPS) to yield copolymers with CAB content as high as 15 mol % hitherto not achieved. The spacer group is shown to provide the twin benefits of enhanced reactivity and solubility in water. The high pK_a at ≥9.90 of these copolymers estimated from potentiometric studies demonstrates packing of AMPS segments as ionic clusters. The higher CAB in copolymer C provides the most densely packed nonpolar microdomains. From fluorescence quenching studies, the cross-linking provided by the cholesterol chains favoring intra- or intermolecular aggregated structures has been established. At the air/solution interface, copolymer C exhibits the most close-packed structures exhibiting "*a*" of 41.2 Å^2/molecule. The effect of neutralization on the adsorption characteristics is investigated.

Introduction

Water-soluble polymeric amphiphiles perform as versatile base components useful in the generation of materials with novel functional properties. The solution structures and the interfacial characteristics of polymeric amphiphiles form the basis in biotechnological applications and interface-related processes. Some examples are the design and modifications of biomaterials,[1−5] solubilization of biologically related compounds like perfumes,[6] and controlled drug delivery systems.[7] Polymers from different copolymer architectures like block and random, consisting of hydrophilic and hydrophobic segments, are shown to exhibit amphiphilic properties.[8] Those consisting of long alkyl side chains provide comblike architectures, and they are highly significant in view of the wide scope in tuning interfacial characteristics and processes. Comblike polymers consisting of ionic segments are expected to respond to different environmental conditions like pH and ionic strength and provide smart materials. These polymers could generate functional latex that forms novel cross-linked structures.[9] They are shown to exhibit different solution structures arising from inter- or intramolecular association. For example, the ionic comonomer consisting of a charged group close to the backbone promotes intermolecular associated structures resembling polysoap as shown in acrylic acid-derived polymers.[10−13] On the contrary, the intrapolymer association gets promoted in 2-acrylamido-2-methyl-1-propane-sulphonic acid (AMPS)-derived polymers with the SO_3H group far away from the backbone.[14] However, in these related polymers, intermolecular associated structures are promoted when the spacer group between the main and side chain is drawn from the ester group.[15]

In these comblike polymers, the flexibility, length, and packing characteristics of the side chain also influence the solution structures and interfacial energy characteristics. The influence of side chain on the interfacial energy characteristics is well demonstrated in alkyl methacrylates and perfluoro methacrylate side chain polymers.[16−18] It is shown that the surface energy of comblike polymers decreases with an increase in the length of alkyl side chain.[19,20] The different solution structures and the adsorption characteristics as controlled by the copolymer composition and their scope in miniemulsion polymerization reaction have been demonstrated in octadecyl methacrylate (ODMA)−acrylic acid (AA) derived polymers.[21,22]

Water-soluble polymeric amphiphiles with comblike structures are highly demanding from the perspectives of synthetic strategies and functional characteristics. They perform as effective steric stabilizers at the interface and could form stable colloidal dispersions or emulsion phase structures.[23,24] It is noteworthy that emulsion phase structures are gaining popularity as templates in the generation of nanomaterials.[25] To employ these polymeric amphiphiles in the formation of emulsions, the understanding of solution structures and interfacial adsorption characteristics of the polymers is essential. We have chosen to design water-soluble polymers consisting of AMPS ionic segments in view of strong acidic functional group capable of withstanding variations in microenvironment. In our series of systemic work on AMPS-derived polymers, we observed that the copolymer composition and the nature of the side chain provide control over the solution structures and adsorption at the air/solution interface. To illustrate, the copolymers consisting of 0.9:0.1 mol % AMPS:ODMA undergo negligible adsorption at the air/solution interface in contrast to those consisting of octadecyl maleate or maleamic side chain showing adsorption contributing to lowering of the surface tension of water to about 48 ± 2 mN/m at 25 °C.[26] In this study, we have chosen to design polymers consisting of cholesterol mesogen in the side chain. We have chosen cholesterol because of some unique characteristics of the cholesterol ring. It is shown that cholesterol brings about organization of lipids significant in membrane behavior.[27] The effect of cholesterol on the ordering of fatty acids with chain length in the range of C_{12}−C_{16} into lamellar structures has been demonstrated. The novel vesicular latex provided by the cholesterol chain attached to the maleimide group through a spacer has been recently established by Menger et al.[28] The importance of cholesterol-derived surfactants in view of biological origin, typical liquid crystalline (LC) and chiral

* Corresponding author. Phone: +91-44-24911386. Fax: +91-44-491-15-89. E-mail: gitsri@hotmail.com.

10.1021/bm061235r CCC: $37.00 © 2007 American Chemical Society
Published on Web 04/11/2007

behavior, has been well brought out in the review on sterol surfactants by Folmer et al.[29] Water-soluble cholesterol derived simple surfactants consisting of a sulfonate group and capable of forming micellar assemblies have been recently reported.[30] Cholesterol−PEG derivatives have been shown to provide suitable LC templates in the generation of nanosize semiconductor materials.[31] In view of the rigidity of the sterol ring imposing restrictions on reactivity, and highly hydrophobic characteristics, the synthesis of water-soluble derivatives consisting of significant amount of cholesterol has been a great challenge. Such copolymers might perform as novel materials and even aid in the solubilization of cholesterol. By the use of spacer groups drawn from hexanoic acid derivatives, the scope for incorporation of significant level of cholesterol side chain has been demonstrated.[32] However, these copolymers were found to exhibit limited solubility at a maximum of 0.1 wt % depending on the nature of the ionic comonomer and the spacer group. Thus, it could be realized that water-soluble polymers consisting of a possible higher cholesterol side chain and exhibiting better solubility hitherto not achieved demand alternate synthetic strategies. For this, we have identified a new spacer group, 4-amino butyric acid, in view of its dual merits of medium polar characteristics due to amino and carboxyl groups, and spacer effect of the C_4 chain. In this study, we have demonstrated the effect of the spacer group in promoting the incorporation of cholesterol side chain comonomer in the AMPS-derived copolymers and solubility in water. We report here the design of three sets of copolymers consisting of a maximum of 15 mol % cholesterol side chain and the organization behavior of these surfactants. We aim to understand the role of the cholesterol side chain in controlling the solution structures and interfacial adsorption characteristics. As surface tension serves as a useful parameter, we have chosen to use tensiometry to draw information on the adsorption characteristics. For the solution structure investigations, the well-known fluoroprobe technique has been employed. The neutralization behavior of these copolymers has been investigated to understand the microenvironment of the AMPS segments in these polymers.

Experimental Section

Materials. 2-Acrylamido-2-methyl-1-propanesulfonic acid (AMPS) 99%, cholesterol 99%, 4-amino butyric acid 99%, dimethyl amino pyridine (DMAP), and acryloyl chloride from Aldrich were used as received without further purification. Dimethylformamide, chloroform, methanol, triethyl amine (TEA), and hexane solvents were of HPLC grade from s.d. fine chemicals, India. Azo-bis(isobutyronitrile) (AIBN) was recrystallized twice from methanol and used. Pyrene 98% from Lancaster was used as received. *N*-Cetylpyridinium chloride (CPC) from Aldrich was recrystallized twice from ethanol and used.

Synthesis of Cholesteryl Acrylamido Butyrate (CAB). CAB was synthesized using a simple procedure adopting two steps as given in Scheme 1. In the first step, cholesterol was converted into an amino acid derivative, by reacting equal moles (1:1) of cholesterol and amino butyric acid in the presence of dimethyl amino pyridine catalyst for a period of 24 h at 60 °C in methanol. The synthesized amino acid derivative was reacted with 3 mol of acryloyl chloride in the presence of triethyl amine at 5 °C for 24 h in chloroform. The product was isolated by repeated washing with water and was recrystallized using methanol. Yield: 85%. Purity: 95%.

Synthesis of AMPS−CAB Copolymers. Copolymers of AMPS−CAB were synthesized by the solution polymerization technique in dimethyl formamide using AIBN initiator at 60 °C for a period of 24 h, employing different feed compositions of the monomers, wherein the composition of CAB was varied in the range of 10−50 mol %.

Scheme 1. Schematic Representation of CAB Synthesis

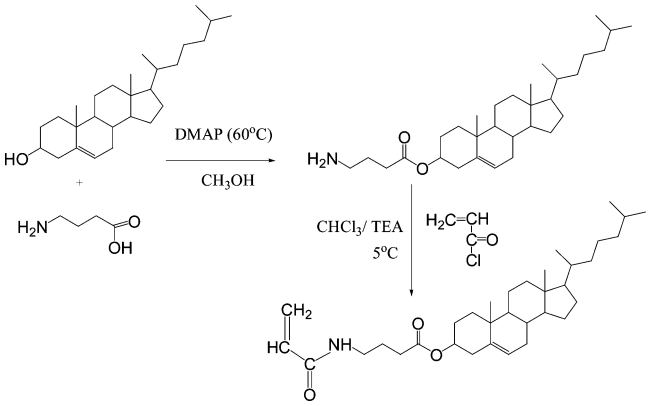

Scheme 2. Schematic Presentation of Copolymers

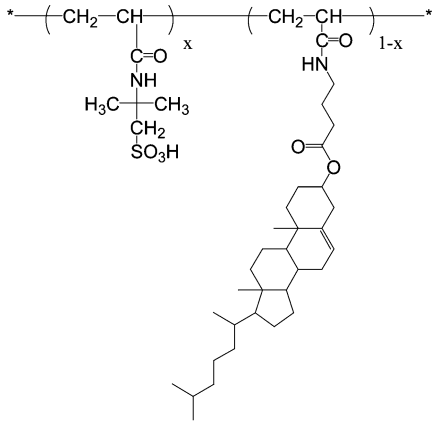

x = 0.85-0.95m; 1-x =0.05-0.15m

The schematic representation of the copolymers is presented in Scheme 2. The composition of the copolymers has been estimated from ^{1}H NMR spectroscopy using the characteristic integral values of the respective monomers. The molecular weight of the polymers was estimated from the single point method using viscometry.[33] The solvent of 0.2 M phosphate buffer solution containing 50% (v/v) acetonitrile was used.[34] The viscosity average molecular weight was calculated from the intrinsic viscosity, fitting the reported Mark−Houwink parameters, K and α values of 3.65×10^{-5} mL/g and 0.77, respectively, estimated for AMPS-derived polymers in Mark−Houwink relation.[35]

Fluorescence. Fluorescence spectra were recorded with a Varian (model Cary Eclipse) spectrophotometer. All measurements were performed at ambient temperature. The slit width of excitation and emission was kept at 5 nm during measurements. The excitation wavelength (λ) was set at 337 nm. The ratio of the intensities of the third I_3 (384 nm) to first I_1 (373 nm) vibronic peak of the fluorescence spectrum of the pyrene probe was used as an estimate of the micropolarity of the pyrene microenvironment.[36] As pyrene exhibits the least solubility in water (1×10^{-7} M), a required volume of stock solution of pyrene in methanol (1×10^{-4} M) was pipetted out into a standard flask, and a thin film of pyrene was deposited on the side of the flask through evaporation of solvent by bubbling N_2 gas. The effective concentration of pyrene was maintained at 1×10^{-6} M in all of the solutions. In the experiments for estimation of aggregation number [N], *N*-cetylpyridinium chloride (CPC) was employed as the quencher, wherein the effective concentrations of the polymer were 8.96×10^{-4}, 5.37×10^{-3}, and 2.2×10^{-2} M for polymer A, 8.36×10^{-4}, 6.27×10^{-3}, and 1.67×10^{-2} M for polymer B, and 3.92×10^{-3} and 7.84×10^{-3} M for polymer C. The fluorescence emission intensities of pyrene were measured for different concentrations of quencher. The plot of the logarithm of the ratio of emission intensities of pyrene in the absence (I_0) and the presence (I) of the quencher versus concentration of quencher was used to assess the applicability of the

modified Stern−Volmer equation in the estimation of the mean aggregation number [*N*].[37]

Neutralization Behavior. pH measurements were carried out with a digital pH-mV meter from Elico LI 120, India. The pH meter was standardized with a buffer solution of pH 4.0 and 9.2. All measurements were done at 25 ± 0.1 °C. A 0.1% solution of the polymers in water was titrated with 0.01 N NaOH. The degree of neutralization (α) defined as the fraction of acid group neutralized was determined for each addition of titrant using the relationship $\alpha = C_{A^-}/C_{HA}$, where C_{A^-} is the concentration of the neutralized acid group and C_{HA} is the total concentration of acid group in the sample.[38] pK_a, which is more informative than the pH curves, was estimated with the well-known Henderson−Hasselbalch equation.

$$pK_a = pH + \log[(1 - \alpha)/\alpha] \quad (1)$$

Surface Tension Estimation. Surface tension measurements were performed for all polymers as a function of concentration ranging from 1×10^{-4} to 0.1 M at different pH of 3.2 and 10.5. The surface tension for the polymers was estimated at 25 °C with a GBX 3S tensiometer from France, with an accuracy of 0.01 mN/m. A platinum du Nuoy ring was used as the probe and standardized with milli-Q water. The reported values are the average of at least three measurements and represent the equilibrium surface tension values.

Interfacial Tension Measurements. Interfacial tension measurements were performed at the hexane/water interface in the presence of polymers at pH 3.2 and 10.5, on a GBX 3S tensiometer at 25 ± 0.1 °C using a platinum du Nuoy ring as the probe. The concentration of the polymers was varied from 1×10^{-4} to 0.1 M. In a typical measurement, 50 mL of water containing a fixed concentration of the polymer was taken, and 25 mL of hexane was added on top of the aqueous phase. The rising of stage with hexane/water sample was enabled and controlled by a built-in microprocessor and stopped automatically as soon as the ring came into contact with the hexane phase. The reported values are the average of at least three estimations, and they represent the equilibrium values.

Optical Microscopy. Optical microscopy was performed on an Olympus BX 50 model microscope over thin films of copolymers. The polymers were coated on a circular cover slip by the dip coating method employing 0.1% of the polymer solution. The coated slips were air-dried, taking care to avoid contamination.

Transmission Electron Microscopy (TEM). The copolymers B and C were investigated for the microstructures on Zeiss TEM of the type Energy Filtering (EF) TEM from Germany. The polymer samples were dissolved in ethanol and deposited on a copper grid. After the samples were dried, staining agents of uranyl acetate and lead citrate were added, dried, and taken up for analysis. TEM investigations were performed to view the microphase-separated structures and the possible changes in such structures with composition of the copolymers.

Results and Discussion

Synthesis and Characterization of Copolymers with Cholesterol Mesogen. As a means of overcoming the steric effect due to a rigid cholesterol ring restricting the incorporation in copolymer, a new monomer has been designed. For this, 4-amino butyric acid has been identified. This is attached to a cholesterol ring through ester linkage and to the main polymeric chain through amide. We have chosen this spacer group for its polar characteristics, which are expected to exhibit interaction with water. Also, this amino acid spacer group has biological significance as a neurotransmitter. The ^{1}H NMR spectrum of the monomer (CAB) (Scheme 1) is presented in Figure 1. The characteristic peak assignments are as follows: δ 0.68 ppm (s) CH_3 of cholesterol; δ 1−2.4 ppm CH_2 and ring protons; δ 1.9 ppm (p) CH_2 of amino butyric acid; δ 2.3 ppm (t) CH_2COO of amino butyric acid; δ 2.8 ppm (t) CH_2NH of amino butyric acid; δ 4.96 ppm (b) NHCO of CAB; δ 5.3 ppm (d) C═CH of cholesterol; and δ 5.8−6.4 ppm of acrylate double bonds. The CAB has been estimated to exhibit 95% purity as observed from the ^{1}H NMR integrals for acrylate double bond and the CH_2-NH proton of the amino butyrate group. The monomer is found to be soluble in a wide range of solvents except water. In view of good solubility of AMPS and CAB in DMF, the copolymerization reactions were performed in DMF wherein the total concentration of the monomers was maintained as 30%. The copolymers were precipitated into diethyl ether and purified by the solvent extraction method. Three sets of copolymers have been designed using feed compositions of the monomers in mole ratios of (1) 0.90:0.10, (2) 0.75:0.25, and (3) 0.50:0.50 mol %. All copolymers were formed in a good yield of 80%. The copolymers have been characterized via the ^{1}H NMR method. The ^{1}H NMR peak assignments are as follows: δ 0.68 ppm (s) CH_3 of CAB; 1−2.4 ppm CH_2 and ring protons of CAB; δ 1.53−1.67 ppm, $-C-(CH_3)_2$ of AMPS; δ 1.9 ppm (p) $-CH_2$ of CAB; δ 2.3 ppm (t) CH_2COO of CAB; δ 2.8 ppm (t) CH_2-NH of CAB; δ 2.82−2.96 ppm $-CH_2$ of AMPS; δ 4.96 ppm (b) NHCO of CAB; δ 5.3 ppm (d) C═CH of CAB; and δ 8.2 ppm NH of AMPS. For the estimation of composition, the well-separated peaks at δ 8.2 ppm due to AMPS and δ 0.68 ppm from CAB have been chosen. Accordingly, the composition of the copolymers has been estimated as presented in Table 1. It could be seen that, under the conditions of the copolymerization reactions, the copolymer composition falls in line with the feed composition, although it does not exactly match. This shows that the new monomer CAB exhibits good reactivity with AMPS, and this monomer indeed promotes incorporation of cholesterol mesogen in the copolymer effecting as high as 15 mol %, which was not possible with simple cholesterol monomer.[34,39,40] The copolymers exhibit molecular weight of the order of 10^5 as estimated from single point viscosity. All copolymers were found to be soluble in water up to a maximum limit of 5 mg/mL. The solutions in water with maximum

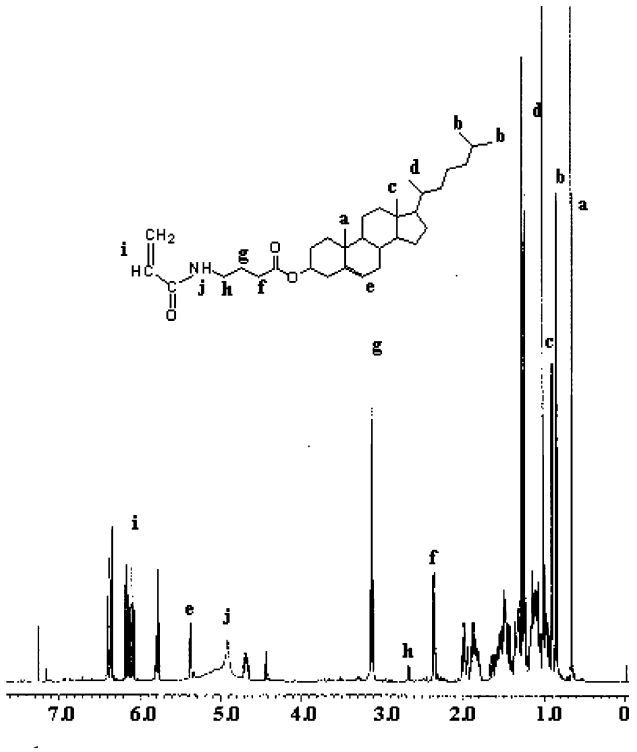

Figure 1. ^{1}H NMR spectrum of the monomer CAB in $CDCl_3$ at 500 MHz.

Table 1. Synthesis and Characterization of the Copolymers

	composition (AMPS:CAB) mole fraction			
system	in feed	estimated, ^{1}H NMR	segmental molecular weight	molecular weight $\times 10^5$ (single point viscosity)
A	0.90:0.10	0.95:0.05	223	1.0
B	0.75:0.25	0.90:0.10	239	1.4
C	0.50:0.50	0.85:0.15	255	2.9

concentration of 5 mg/mL remain transparent as shown from a constant high transmittance at 500 nm. From the work of Morishma et al. on related ionic polymers with cholesterol mesogen, it could be seen that water-soluble polymer consisting of a maximum of 0.001 or 5 mol % and exhibiting solubility up to 0.1% was achieved. To the best of our knowledge, we feel that the reported copolymer consisting of a significant proportion to an extent of 15 mol % and exhibiting water solubility at about 0.5% is the first of its kind. It is worth mentioning here that these copolymers exhibit better solubility under alkaline conditions up to a maximum of 10 mg/mL.

Neutralization Behavior. The microenvironment of the ionic groups plays a significant role in influencing the neutralization behavior, and this is well demonstrated in acrylic acid derived polymers.[41,42] In view of strong acidic functionality, the sulfonic acid group of AMPS forming the ionic segment of the copolymers is expected to exhibit complete dissociation. However, the neutralization behavior is expected to change depending on the microenvironment of the AMPS segments. We have estimated the degree of neutralization (α) at different pH from the potentiometric titration method. Applying the Henderson−Hasselbalch equation (eq 1), pK_a was estimated at different pH. The plot of pH and pK_a versus α of the three copolymers A, B, and C is presented in Figure 2a and b. Table 1 can be referred to for the designation of the copolymers. The results on the dissociation behavior for the copolymers and the homopolymer, PAMPS, are presented in Table 2. From the curves (Figure 2), it could be seen that these copolymers exhibit resistance to neutralization. Also, in these sets of copolymers, we find that the neutralization behavior is different. The copolymer A consisting of 5 mol % CAB exhibits a more facile neutralization process, typical of a strong acid group over a narrow pH range of 3.5−4.0 until it reached an α of 0.30. After this, over a broad pH range of 4.0−9.0, a negligible change in α was observed. This behavior is indicative of strong resistance to neutralization. We believe the presence of AMPS segments as ionic clusters enabled by the coil structures of the polymer chain contributes to electrostatic repulsion on neutralization, thus accounting for the observed behavior. Over the pH range of 4.0−9.0, the solution structure remains almost unaltered. On further increase in pH, α increases sharply and reaches the value of 1.0, and this is effected with an increase in pH from 9.0 to about 10.5. This implies that the polymer chain undergoes continuous expansion on neutralization, and the most stable expanded conformation as a means to overcome the electrostatic repulsion among the partially neutralized AMPS segments is attained at pH $\geq$ 9.0, that is, after reaching an α of about 0.40. On the contrary, the enhanced resistance to neutralization could be seen from the lower α at 0.13 and 0.02 at pH 7.0 for the copolymers B and C, respectively. In these copolymers, α increases sharply from about 0.30 to 1.0, over the very narrow pH range of 10.0−10.5. It could be seen that these copolymers show typical characteristics of resistance to neutralization similar

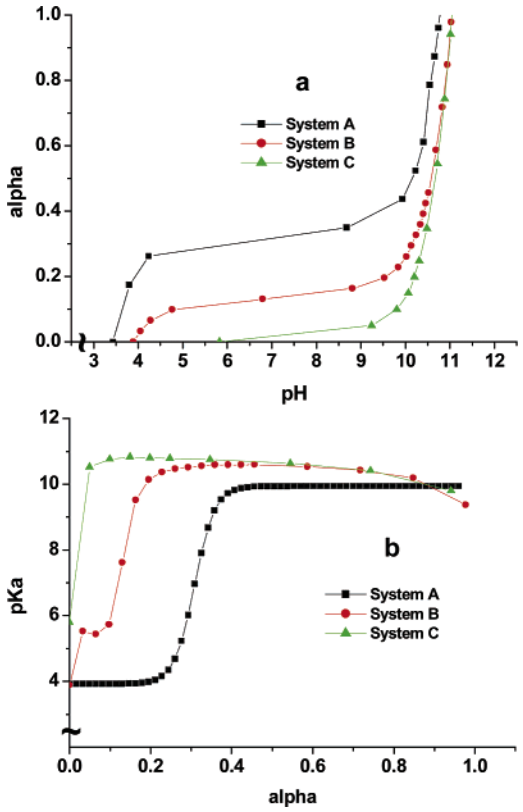

Figure 2. Plot of (a) pH versus α and (b) α versus pK_a from potentiometric titration performed on 0.1% aqueous polymer solution in water for the copolymers A, B, and C, temp 25 °C.

Table 2. α and pK_a Values of the Copolymers and PAMPS at Different pH

system	pH	α	pK_a
A	7.00	0.316	7.320
	10.14	0.500	10.11
	10.50	0.691	9.920
	10.78	0.999	8.825
B	7.00	0.132	7.460
	10.50	0.438	10.58
	10.58	0.500	10.53
	11.04	0.999	9.044
C	7.00	0.021	8.080
	10.50	0.354	10.777
	10.65	0.500	10.650
	11.04	0.999	9.044
PAMPS	7.00	0.170	5.10
	10.20	0.500	10.20
	10.50	0.850	9.94
	10.70	0.999	8.70

to the homopolymer PAMPS, which showed a high pK_a of 10.20 at an α of 0.5 (Table 2).[26] From these results, it could be understood that the presence of AMPS as ionic clusters underlies this feature of resistance to neutralization, contributing to high pK_a with respect to both homopolymer and copolymers. However, the difference in the neutralization behavior among the copolymers as suggested from Figure 2 suggests that the cholesterol mesogen content in the copolymer probably influences the conformation of the coil structures that could modify the packing characteristics of ionic clusters of AMPS. With the increase in cholesterol comonomer to 15 mol % as in copolymer C, almost negligible neutralization occurs at pH 7.0 in contrast to copolymer A, wherein it is estimated as 0.31 (Table 2). It is thus implied that in these copolymers, the cholesterol mesogen

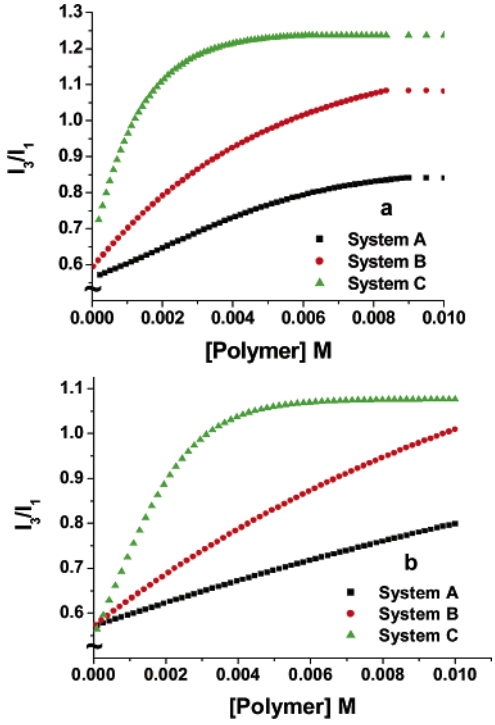

Figure 3. Plot of I_3/I_1 emission intensity ratio of pyrene in aqueous solution of copolymers versus the concentration of the aqueous polymer solution at (a) pH 3.2 and (b) pH 10.5, temp 25 °C.

promotes coil structures consisting of close-packed ionic clusters of AMPS segments. It is interesting to note that almost similar structures consisting of ionic clusters of AMPS could be observed in the homopolymer. In all of these polymers, it could be visualized that, on increasing the pH, the coil structures undergo expansion and attain the expanded conformation, whereby the loosely packed ionic clusters of AMPS become more amenable for neutralization. The homopolymer and the copolymers show 50% and 100% neutralization over a narrow pH range of 10.0−11.0.

Microstructures of Polymer Solution from Fluoroprobe Investigations. The microenvironment of the aqueous solutions of copolymers in the aspect of micropolarity has been investigated using a well-established fluoroprobe technique.[36] The ratio of emission intensity, I_3 (384 nm)/I_1(373 nm), of pyrene employed as an external probe in copolymer solutions has been used to draw information on the micropolarity. These measurements have been carried out over the concentration range of 5 $\times$ 10^{-4} to 0.01 M (0−2.5 mg/mL). Such measurements were also performed at pH 10.5, wherein these copolymers exhibit an α at about 0.4−0.7, to find the effect of neutralization on the micropolarity. The plots of I_3/I_1 at different concentrations for the copolymers at pH 3.2 and 10.5 are presented in Figure 3a and b. At pH 3.2, wherein $\alpha = 0$, it is observed that I_3/I_1 progressively increases with an increase in the concentration of the polymer solution. At zero concentration of the copolymer, I_3/I_1 has been estimated as about 0.62, which is in agreement with the reported value in water. Considering the I_3/I_1 number serves as a direct indicator on the micropolarity, it is observed that with respect to copolymer C, maximum I_3/I_1 at 1.23 was estimated at a concentration $\geq$0.003 M (0.765 mg/mL). The I_3/I_1 value is a direct measure of the nonpolar characteristics of the microdomains. The high I_3/I_1 ratio implies that the solubilization site of the pyrene fluoroprobe is comparatively more nonpolar in copolymer C. From the values of I_3/I_1 ratio estimated at the maximum concentration of 0.01 M, it could be seen that

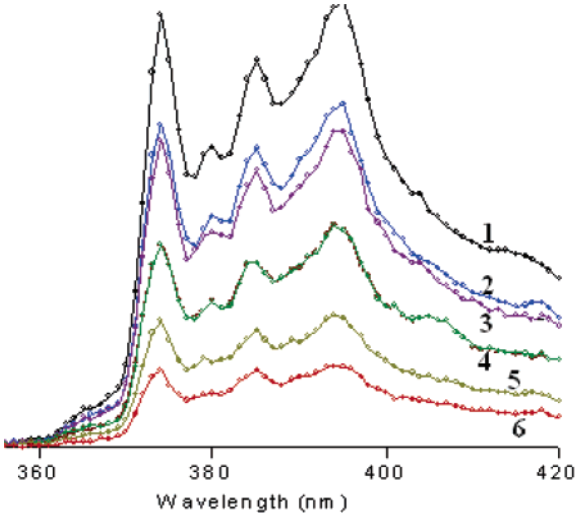

Figure 4. Fluorescence spectral curves of pyrene [1 $\times$ 10^{-6} M, fixed], in the presence of aqueous solution of the copolymer A [2.2 $\times$ 10^{-2} M, fixed], at different concentrations of quencher, CPC. Curves 1−6: −1 $\times$ 10^{-5}, 2.5 $\times$ 10^{-5}, 5 $\times$ 10^{-5}, 7.5 $\times$ 10^{-5}, 1 $\times$ 10^{-4}, and 2.5 $\times$ 10^{-4} M, respectively, temp 25 °C.

the nonpolarity of the microdomains follows the order copolymer C > B > A. From our estimations on I_3/I_1 in the aqueous solution of PAMPS, it was found that I_3/I_1 showed a negligible change with concentration of the polymer.[26] This suggests that, in these copolymers, the side chain cholesterol mainly contributes to microdomain formation. Under these conditions, as compared to the composition of the copolymers, the density of nonpolar domains increases with an increase in cholesterol component. At pH 10.5, I_3/I_1 values are comparatively lower for all three copolymers, although the changes are maximum with respect to copolymer A and the least with copolymer C. In copolymer A at pH 10.5, α approaches almost 1.0 in contrast to copolymers B and C where it is around 0.5. The results indicate the promotion of electrostatic interaction on neutralization, that is, on increasing α, and favors expanded conformation. By this, compactness of the nonpolar microdomains is reduced significantly. These results are in support of the results from the neutralization behavior as discussed above.

Estimation of Aggregation Number. The well-established fluorescence quenching method has been adopted to estimate the average aggregation number [N]. The use of the fluorescence quenching method requires compliance of various conditions involving fluorescence kinetics and quenching mechanism. This method demands the Poisson model for the distribution of probe and quencher in an aggregate. In the present investigations, we have employed the well-established surface-active CPC quencher. The quenching experiments were performed on polymer solutions of concentrations 8.96 $\times$ 10^{-4}, 5.37 $\times$ 10^{-3}, and 2.2 $\times$ 10^{-2} M for polymer A, 8.36 $\times$ 10^{-4}, 6.27 $\times$ 10^{-3}, and 1.67 $\times$ 10^{-2} M for polymer B, and 3.92 $\times$ 10^{-3} and 7.84 $\times$ 10^{-3} M for polymer C. The representative fluorescence quenching spectral curves in the presence of copolymer A and different concentrations of quencher are presented in Figure 4. The modified Stern−Volmer plots for the polymers are presented in Figure 5. The validity of the Poisson distribution model and extended Stern−Volmer equation in the investigated system is provided by the plot of the logarithm of the emission intensity ratio of pyrene in the absence (I_0) and the presence (I) of quencher (ln I_0/I) versus the concentration of the quencher ([CPC]). It could be seen that all of these plots are linear and thus demonstrate the compliance of the modified Stern−Volmer equation, and ensure solubilization of CPC in polymer micelle,

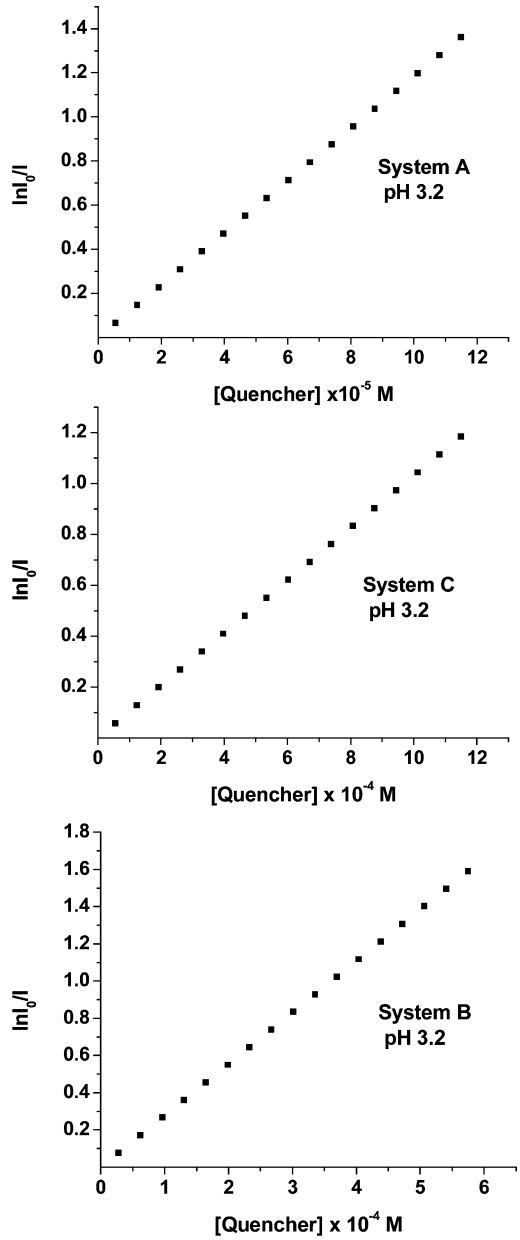

Figure 5. Plot of ln I_0/I versus concentration of quencher, CPC, [pyrene] = 1×10^{-6} M fixed. Concentrations of the polymers A, B, and C are 2.2×10^{-2}, 1.67×10^{-2}, and 7.8×10^{-3} M, respectively, temp 25 °C.

which serves as the predominant host for the probe, pyrene. The linear plots passing through the origin are indicative of the diffusion-controlled quenching mechanism obeying the static quenching mechanism. [*N*] is then estimated, applying the extended Stern−Volmer equation developed by Turro and Yekta. The slope of the plot is related to the aggregation number as follows:

$$\ln I_0/I = [\text{CPC}]/[\text{micelle}]$$

$$[\text{micelle}] = [\text{polymer}] - [\text{CMC}]/[\text{N}] \qquad (2)$$

where the concentration of the polymer is expressed in mol/L. In view of the least tendency of poly(AMPS)[15] to form microdomains, it is more meaningful to consider that [*N*] is indicative of the number of cholesteryl residues of the polymer chain involved in the aggregate structure formation. Under conditions of very low critical micelle concentration (CMC) almost approaching zero that could be anticipated for polymeric amphiphiles, the estimate of [*N*] was performed. The slope and relative error value have been calculated by the least-square method. A good linearity was obtained with a relative 2−3% error in the slope. The aggregation numbers thus estimated are presented in Table 3. We have chosen to analyze our results by comparing the number of CAB chains present in a single polymer chain with those participating in the aggregated structure/hydrophobic microdomain formation. It is interesting to observe that aggregation number varies significantly among the three polymers. Polymer A consisting of 5 mol % cholesterol side chain segments tends to promote aggregation among cholesterol chains as a function of concentration. From Table 3, it could be seen that [*N*] increases from 18 to 74, that is, about 4 times on increasing the concentration from 8.96×10^{-4} to 5.37×10^{-3} M. In decimolar concentration (2.2×10^{-2} M), there is still an indication for the growth of aggregated structure contributing to [*N*] of 233, that is, about a 13-fold increase. From the number of cholesteryl chains computed from the molecular weight and mole fraction of the cholesterol component in the polymer, it could be seen that polymer A consisting of about 9.5 cholesterol chains tends to promote intermolecular aggregated chains among about two polymeric chains. This polymer at the concentration of 2.2×10^{-2} M could form gigantic aggregated structures, promoting association among about 25 polymeric chains. This trend of intermolecular association is in accordance with the reports of Morishma et al.[34,39,40] on related copolymers. On the contrary, polymers B and C consisting of 10 and 15 mol % cholesterol segments show different behavior. Polymer B shows a maximum 2-fold increase in aggregation number with concentration; that is, [*N*] increases from about 18 to 36 on increasing the concentration from 8.36×10^{-4} to 1.67×10^{-2} M. Comparing the aggregation number with the number of cholesterol chains in one polymeric chain, polymer B could be considered to promote almost unimolecular aggregated structure at all concentrations. Interestingly, in polymer C, [*N*] remains almost invariant with concentration. Thus, [*N*] is estimated as 22 and 24 at concentrations of 3.92×10^{-3} and 7.84×10^{-3} M, respectively. Polymer C promotes intramolecular aggregated structures, and the number of microdomains in one polymeric chain is about 4. Generally, an increase in hydrophobic side chain component is expected to promote intermolecular aggregated structure formation. The opposite trend observed in this copolymer C suggests that the rigid sterol ring in the side chain plays a significant role in influencing the aggregated structure formation. It is possible that the steric effect becomes more pronounced with the cholesterol component in the side chain. The competition among different forces arising from electrostatic interaction due to

Table 3. Estimation of Aggregation Number [*N*] Using Fluorescence Quenching Method for the Copolymers at Different Concentrations

system	concentration of the copolymers (M)	[*N*] at pH 3.2	no. of cholesteryl chains
A	8.96×10^{-4}	18	9.50
	5.37×10^{-3}	74	
	2.20×10^{-2}	233	
B	8.36×10^{-4}	18	26.70
	6.27×10^{-3}	28	
	1.67×10^{-2}	36	
C	3.92×10^{-3}	22	85.14
	7.84×10^{-3}	24	

AMPS segment, steric, and hydrophobic forces from cholesterol side chain segments seems to control the aggregated structure formation. The presence of cholesterol segment at a very small level of 5 mol % is able to promote the hydrophobic effect, and this favors intermolecular aggregated structure formation. At 10 mol % level of cholesterol in the polymer as in polymer B, almost unimolecular micellar-like structures are promoted. With further increase in cholesterol to 15 mol %, the combined steric and hydrophobic effects become more dominating features, and this favors intramolecular aggregated structure formation. The distribution of about four microdomains that are well separated and consisting of about 23 ± 1 cholesterol chains in one polymeric chain accounts for the higher density of nonpolar domains in polymer C. The fluorescence quenching experiments demonstrate that cholesterol side chain performs as an efficient cross-linking agent, providing intra- and intermolecular association among cholesterol side chains of the same or different polymeric chains as dictated by the hydrophobic and steric effects or, in other words, cholesterol content of the copolymers. Furthermore, these results also rule out the blocky distribution of cholesterol side chains especially in copolymer C, as such a situation would demand linear structures to overcome the steric factor. Under these conditions, intermolecular aggregated structures could be anticipated in line with the reports of McCormick et.al.[11,43,44] This is expected to result in very high [*N*], much greater than the number of cholesterol side chains in one polymer chain, that is, much higher than 85. The much lower [*N*] at about 23 ± 1.3 observed with this copolymer C suggests the statistical distribution of cholesterol chains in the copolymer.

Adsorption Characteristics of the Copolymers at the Air/Solution Interface. It is understood that the nonpolar segment of a simple or polymeric surfactant promotes adsorption at the air/solution interface and effects reduction in the surface tension of water. The estimate of surface tension of aqueous solutions of polymers at different concentrations provides the simplest methodology to draw information on the adsorption characteristics. In these investigations, we have estimated the surface tension of copolymer solutions in water over a concentration range of 1×10^{-4} to 0.1 M. From the neutralization behavior, it is observed that these copolymers exhibit different degrees of neutralization at pH 10.5 (Table 2). We have performed surface tension experiments for these copolymers at pH 3.2 and 10.5 to draw information on the influence of neutralization on the adsorption characteristics. The plots of surface tension (γ) versus concentration in the log scale for the copolymers at different pH are presented in Figure 6. All copolymers exhibit good adsorption at the interface as observed from the continuous decrease in surface tension of water from about 71 ± 0.5 mN/m with concentration. This is in sharp contrast to the behavior reported for the ionic polymeric amphiphiles,[45−48] wherein those polymers form micellar solutions showing the least activity at the interface. In our series of work on similar kinds of polymers, we have observed that the side chain plays a significant role in modifying the electrostatic forces predominant in such ionic polymer systems and influences adsorption characteristics at the interface.[26] For all copolymers at different pH conditions, the pattern of change in γ with concentration follows simple surfactant behavior, showing regions of progressive drop in surface tension with concentration, which remains almost constant at and above a critical concentration. The concentration over which negligible change in γ occurs corresponds to critical aggregation concentration (CAC). The γ corresponding to CAC is termed here as γ_{equ}. The constant γ after CAC suggests the formation of monolayer of the polymer at the interface. Applying the Gibbs adsorption isotherm, eq 3, the surface excess concentration (Γ) and surface area/molecule (a) of the polymer segment have been estimated.[49]

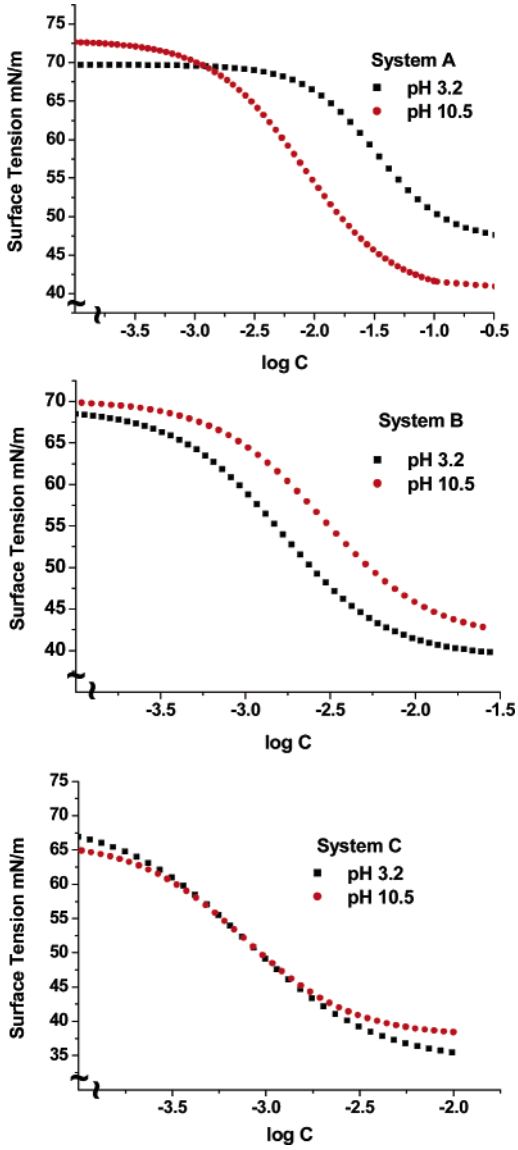

Figure 6. Gibbs adsorption isotherm plots of surface tension (γ) versus log *C* at different pH for the copolymers A, B, and C, temp 25 °C.

$$\gamma = -RT\Gamma \ln C = -2.303RT\Gamma \log C$$

$$a = 10^{23}/N\Gamma \qquad (3)$$

The adsorption characteristics of the copolymers are presented in Table 4. At pH 3.2, it is observed that adsorption at the air/solution interface is favored with increase in cholesterol component in the copolymer as observed from the lowest γ_{equ} at 34 mN/m for the copolymer C against that of copolymer A showing γ_{equ} at 48.1 mN/m. Also, the efficiency of adsorption is the highest with copolymer C as inferred from the maximum surface coverage (Γ) of 4.03×10^{-3} mol/m^2. Copolymer C exhibits the most close-packed structures contributing to a surface area of 41.2 Å^2/molecule. It is known and also we found from our experiments that PAMPS exhibits negligible adsorption at the air/solution interface as observed from very high surface tension of PAMPS solution at a concentration as high as 0.01

Table 4. Surface Area (*a*), Surface Coverage (Γ), and Critical Aggregation Concentration (CAC) of Copolymers A, B, and C at the Air/Solution Interface as a Function of pH from Gibbs Adsorption Isotherm Plots, Temp 25 °C

	CAC (M)		equilibrium surface tension mN/m		surface area/molecule (*a*) (Å²/molecule)		surface coverage (Γ) × 10^{-3} (mol/m²)	
system	3.2	10.5	3.2	10.5	3.2	10.5	3.2	10.5
A	0.20	0.10	48.1	44.6	83.9	41.1	1.98	4.04
B	0.04	0.03	39.1	41.9	56.4	43.0	2.95	3.85
C	0.02	0.01	34.0	40.1	41.2	45.81	4.03	3.62

M, typical of ionic polymers. The significant adsorption behavior observed with these copolymers demonstrates the adsorption of cholesterol side chain at the interface. The results showing enhanced efficiency in adsorption characteristics with copolymer C consisting of 15 mol % cholesterol segment also are in support of this observation. The adsorption characteristics of these copolymers at pH 10.5 are presented in Table 4. For polymer A, wherein α is about 0.691 at pH 10.5, efficiency of adsorption is tremendously improved. This is inferred from a 2-fold increase in Γ to 4.04×10^{-3} mol/m² and about 50% reduction in surface area from 83.9 to 41.1 Å²/molecule. However, it is significant to note that γ_{equ} undergoes a very small decrease to 46.4 mN/m. On the contrary, in copolymers B and C, there is a small drop in surface activity. In polymer C, surface coverage decreases by about 10%, contributing to an increase in surface area by about 9.7%. Interestingly, in all of the copolymers, the γ_{equ} varies within 2−3 mN/m from the mean value at pH 3.2 and 10.5. The α at <0.55> in copolymers B and C although is expected to promote electrostatic forces; by virtue of significant cholesterol segment in these copolymers, surface activity seems affected to a small extent. On the other hand, in polymer A wherein α ≈ 0.69, the promotion of electrostatic repulsion among AMPS segments favors adsorption of the cholesterol segment at the interface providing close-packed structures. These results suggest that it is possible to bring about the most close-packed structures of cholesterol segment at the air/solution interface with the copolymer containing cholesterol segment as low as 5 mol % by suitably manipulating the electrostatic interaction. To the best of our knowledge, literature on adsorption characteristics of related polymers is lacking, and this is the first report. Furthermore, the small change in γ_{equ} within 2−3 mN/m from the mean value at pH 3.2 and 10.5 further supports that the cholesterol segment of the copolymer contributes to adsorption and the manipulation of the electrostatic forces brings about changes in the packing characteristics of cholesterol segment at the interface.

Adsorption Behavior of the Copolymers at the Liquid/Liquid Interface. The adsorption characteristics of surfactants, simple or polymeric at the liquid/liquid interface, provide useful information on the scope for the generation of stable dispersions.[50] In this study, we have chosen water and hexane. The interface between these liquids is distinct with a high interfacial energy at 50.2 mN/m at 25 °C. The adsorption of the copolymer at the interface is expected to contribute to changes in interfacial tension. We have estimated the interfacial tension of the water/hexane interface at different concentrations of the copolymers. These experiments were performed at pH 3.2 and 10.5. The plots of change in interfacial tension (γ_{int}) as a function of concentration of copolymer solutions in log scale are presented in Figure 7. From these plots, one could see that all copolymers effect reduction in γ_{int} with concentration. At and above certain concentration, γ_{int} changes negligibly similar to those observed with the air/solution interface. This pattern indicates the monolayer and equilibrium coverage provided by the copolymer

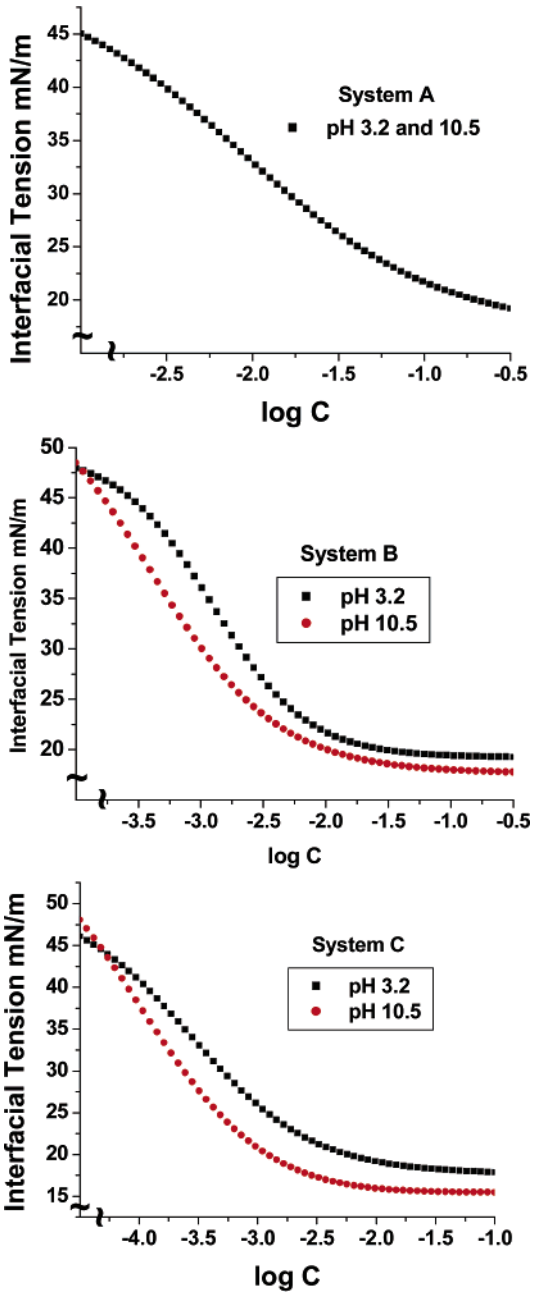

Figure 7. Plot of interfacial tension (water/hexane) (γ) versus log *C* at different pH values for the copolymers A, B, and C, temp 25 °C.

at the interface. We have employed the Gibbs adsorption isotherm equation to estimate the surface coverage (Γ) and surface area (*a*) of the copolymer at the interface. The results on Γ and *a* are presented in Table 5. It is interesting to observe that the adsorption pattern at the liquid/liquid interface is very different from that at the air/solution interface, which implies that the nature of the interface is very important in these studies.

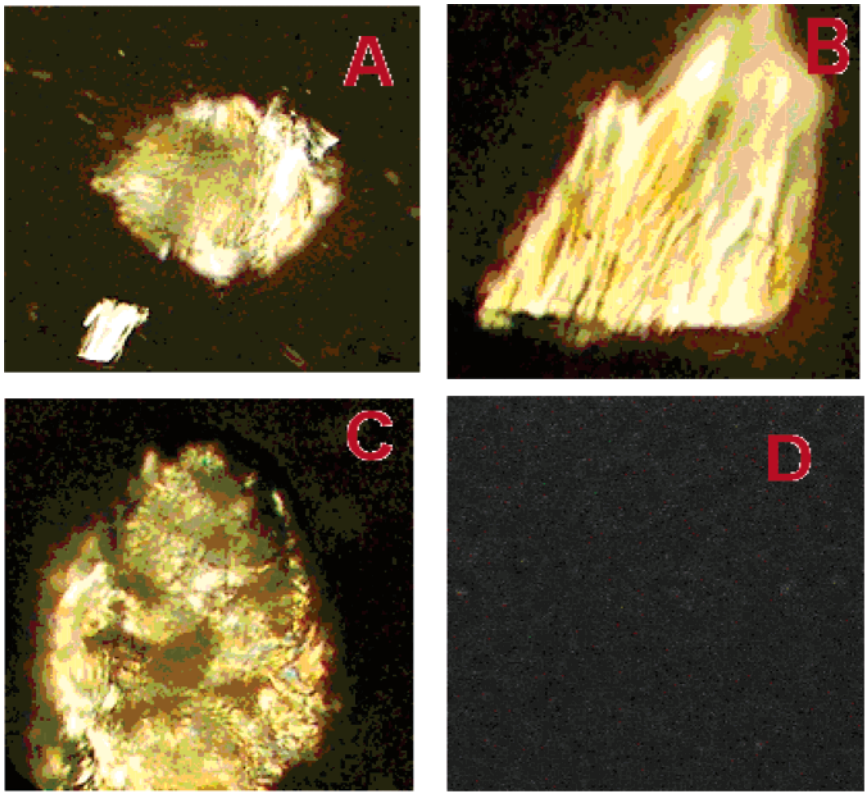

Figure 8. Optical micrographs A−C: copolymers A, B, and C. D: PAMPS at room temperature under cross polarizer, 50×.

Table 5. Surface Area (*a*) and Surface Coverage (Γ) of Copolymers A, B, and C at the Water/Hexane Interface as a Function of pH from Gibbs Adsorption Isotherm Plots, Temp 25 °C

	equilibrium interfacial tension mN/m		surface area/molecule (*a*) (Å²/molecule)		surface coverage (Γ) × 10^{-3} (mol/m²)	
system	3.2	10.5	3.2	10.5	3.2	10.5
A	19.5	19.5	67.8	67.80	2.45	2.45
B	19.5	18.0	51.23	51.08	3.24	3.25
C	18.0	15.0	63.85	47.42	2.60	3.50

At pH 3.2, it could be observed that interfacial tension decreases from about 48.00 ± 1 to 18.75 ± 0.75 mN/m, which remains constant thereafter, in the presence of these copolymers. It is noteworthy to mention here that PAMPS under these conditions does not contribute to significant changes in γ_{int}. From this, it could be considered that changes in γ_{int} are effected mainly due to adsorption of cholesterol segment at the interface. The small difference in minimum constant value, that is, γ_{int} (min) suggests that the cholesterol content of the copolymer does not influence this value. The γ_{int} value serves as an indirect parameter, providing information on the average conformation of the polymer segment at the interface. Based on this, it is implied that the conformation of the cholesterol segment adsorbed at the liquid/liquid interface is almost the same with respect to the three copolymers. However, the adsorption characteristics as inferred from surface coverage and surface area are different for these copolymers. It is observed that copolymer B consisting of 10 mol % cholesterol segments provides the most close-packed structures of cholesterol segment at the interface contributing to the Γ of 3.24 × 10^{-3} mol/m² and the least surface area of 51.23 Å²/molecule. On the contrary, copolymers A and C exhibit a larger surface area of 65 ± 2 Å²/molecule. Based on the cholesterol content, this result could be explained as arising due to inefficient coverage due to a very small cholesterol content at 5 mol % as in copolymer A or loosely packed structures due to the steric factor that could be possible with polymer C in view of the high cholesterol segment at 15 mol %. At pH 10.5, the copolymers A and B do not contribute to significant changes in interfacial adsorption characteristics. Thus, for example, for the copolymer B, surface area changes from 51.23 to 51.08 Å²/molecule, which is almost negligible. Also, the γ_{int} (min) is brought down from 19.5 to 18.0 mN/m, which is about a 5% decrease and not very significant. Interestingly,

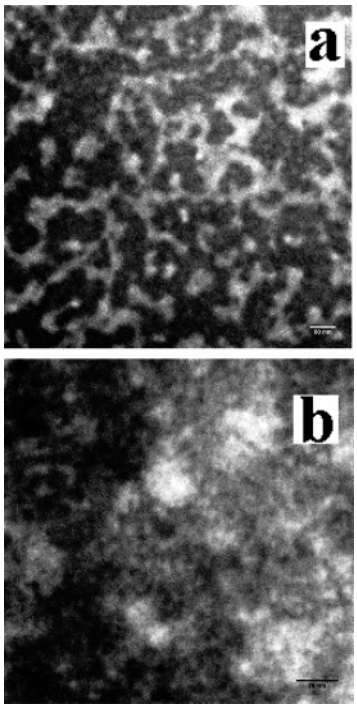

Figure 9. Transmission electron micrograph of the copolymers B (a) and C (b) at 40 and 50 K.

in copolymer C at pH 10.5, improvement in interfacial adsorption characteristics is seen. This is inferred from a decrease in γ_{int} equilibrium to 15 mN/m and excellent drop in surface area by about 30%. The partial neutralization of AMPS segment at pH 10.5 at α 0.35 in copolymer C contributes to significant changes in the adsorption characteristics. It is possible that, under these conditions, the conformation of the adsorbed segments at the interface changes significantly and effects close-packed structures at the interface. It is thus inferred that the optimum level of 10 mol % cholesterol component in the copolymer is able to favor adsorption at the liquid/liquid interface, providing close-packed structures at the interface under a wide range of pH conditions.

Microscopic Studies on Copolymers. *Optical Microscopy.* The optical micrographs of the copolymers viewed under cross polarizers are presented in Figure 8. These studies were performed in comparison with PAMPS homopolymer. However, the homopolymer did not show any distinct features as shown in Figure 8D. It could be seen that all copolymers show strong birefringence under a cross polarizer, and this is indicative of anisotropic features. We strongly believe that cholesterol component in the copolymer accounts for this property. It is observed that cholesteric features are well exhibited in all of the copolymers, and these features are clear in copolymer C consisting of 15 mol % cholesterol segment.

Transmission Electron Microscopy. The microstructures of the copolymers were further studied using TEM. In view of the simplicity of the procedures, these studies were performed using ethanol as solvent. The TEM micrographs of the copolymers B and C at magnifications of 40 and 50 K are presented in Figure 9a and b. It could be seen that copolymer B shows distinct microphase separation with uniform network-like structures. We believe that network-like structures are due to the cholesterol segment of the polymer. In copolymer C, dense and uniform network-like structures could be seen. We strongly feel that this represents the typical cholesteryl chains. The TEM experiments in ethanol provide information on the tendency of the investigated copolymers to form uniform network structures, although these results cannot be considered to support our inferences on the aqueous solution structures established in detail by different techniques.

Conclusions

The new monomer, CAB with cholesterol chain and consisting of a spacer group of 4-amino butyric acid, has been demonstrated to promote copolymerization reaction with AMPS, to provide copolymers with a cholesterol mesogen component as high as 15 mol %. The copolymers exhibit significant solubility in water at 0.5% (wt %) over a wide range of pH values. The copolymers exhibit resistance to neutralization as observed from high pK_a at $\geq$9.90 for α of 0.5, which is explained on the basis of packing of AMPS segments as ionic clusters in the coiled structures. The density of nonpolar microdomains of copolymer solutions increases with cholesterol component as established from the fluoroprobe method. Cholesterol side chain performs as a good cross-linking agent, promoting intra- or intermolecular aggregated structures as established from fluorescence quenching experiments. Interestingly, copolymer C consisting of a higher cholesterol component at 15 mol % promotes intramolecular aggregated structures with the packing of about 23 cholesterol chains in contrast to copolymer A promoting intermolecular aggregated structures. All copolymers exhibit significant adsorption at the air/solution and liquid/liquid interface, providing monolayer coverage at the interface. At the air/solution interface, copolymer C exhibits the most close-packed structures, exhibiting "*a*" of 41.1 Å^2/molecule. By tuning the electrostatic interaction, it is demonstrated that it is possible to enhance the efficiency of adsorption at both the air/solution and the liquid/liquid interfaces. From optical microscopic studies, the copolymers are shown to exhibit strong birefringence under cross polarizers. TEM micrographs show network-like structures typical of cholesterol chains.

Acknowledgment. We thank Dr. A. B. Mandal, Acting Director, CLRI, India, for his constant encouragement and permission to publish this paper. The support of Dr. B. S. R. Reddy, Deputy Director, CLRI, is acknowledged. K.C. thanks CSIR, India, for a fellowship. G.B. thanks DST, India, for the partial financial assistance through grant SR/S1/PC14/2004. The support of Dr. D. Khushalani, TIFR, in the TEM experiments is gratefully acknowledged.

References and Notes

(1) Yekta, A.; Duhamel, J.; Brochard, P.; Adiwidjaja, H.; Winnik, M. A. *Macromolecules* **1993**, *26*, 1829.
(2) Kumacheva, E.; Rharbi, Y.; Winnik, Y. M. A.; Guo, L.; Tam, K. C.; Jenkins, R. D. *Langmuir* **1997**, *13*, 182.
(3) Zhang, Y. B.; Wu, C.; Fang, O.; Zhang, Y. X. *Macromolecules* **1996**, *29*, 2494.
(4) McCormick, C. L.; Middleton, C. L. *Polym. Mater. Sci.* **1987**, *57*, 700.
(5) Chen, J.; Jiang, M.; Zhang, Y.; Zhou, H. *Macromolecules* **1999**, *32*, 4861.
(6) *Principles of Polymer Science and Technology in Cosmetics and Personal Care*; Goddard, E. D., Gruber, J. V., Eds.; Marcel Dekker: New York, 1999.
(7) Bock, J.; Varadaraj, R.; Schulz, D. N.; Maurer, J. J. In *Macromolecular complexes in Chemistry and Biology*; Dubin, P. L., Bock, J., Davies, R. M., Schulz, D. N., Thies, C., Eds.; Springer-Verlag: Berlin and Heidelberg, 1994; p 33.
(8) Foster, S.; Antonietti, M. *Adv. Mater.* **1998**, *10*, 195.
(9) Kanouni, M.; Rosano, H. L.; Naouli, N. *Adv. Colloid Interface Sci.* **2002**, *99*, 229.
(10) Wang, T. K.; Iiopoulos, I.; Audebert, R. In *Water Soluble Polymers*; Shalaby, S. W., McCormick, C. L., Butler, G., Eds.; ACS Symposium Series 467; American Chemical Society: Washington, DC, 1991; p 218.
(11) Kramer, M. C.; Steger, J. R.; Hu, Y.; McCormick, C. L. *Macromolecules* **1996**, *29*, 1992.
(12) Cochin, D.; Candau, F.; Zana, R. *Macromolecules* **1993**, *26*, 5755.
(13) Stranss, U. P.; Gershfeld, N. L. *J. Phys. Chem.* **1956**, *60*, 577.
(14) Morishima, Y.; Nomura, S.; Ikeda, T.; Seki, M.; Kamachi, M. *Macromolecules* **1995**, *28*, 2874.
(15) Noda, T.; Morishima, Y. *Macromolecules* **1999**, *32*, 4631.
(16) Luning, J.; Stohr, J.; Sorg, K. Y.; Hawker, C. J.; Iodice, P.; Nguyen, C. V.; Yoon, D. Y. *Macromolecules* **2001**, *34*, 1128.
(17) Gibbs, J. H.; Smyth, C. P. *J. Am. Chem. Soc.* **1951**, *73*, 5115.
(18) Foret, L.; Wierger, A. *Phys. Rev. Lett.* **2001**, *86*, 5930.
(19) Mol, E. A. L.; Shindler, J. D.; Shelaginov, A. N.; Dejeck, W. H. *Phys. Rev.* **1996**, *54*, 536.
(20) Stoeke, T.; Mach, P.; Grantz, S.; Huang, C. *Phys. Rev.* **1996**, *53*, 1662.
(21) Baskar, G.; Ramya, S.; Mandal, A. B. *Colloid Polym. Sci.* **2002**, *280*, 886.
(22) Baskar, G.; Landfester, K.; Antonietti, M. *Macromolecules* **2000**, *33*, 9228.
(23) Kusters, J. M. H.; Napper, D. H.; Gilbert, R. G.; German, A. L. *Macromolecules* **1982**, *25*, 7043.
(24) Prima, I. *Polymeric Surfactants, Surfactant Science Series No. 42*; Marcel Dekker: New York, 1993.
(25) Romoscanu, A. I.; Mezzenga, R. *Langmuir* **2006**, *22*, 8770.
(26) Chandrasekar, K.; Baskar, G. *J. Polym. Sci., Part A: Polym. Chem.* **2006**, *44*, 314.
(27) Ouimet, J.; Lafleur, M. *Langmuir* **2004**, *20*, 7474.
(28) Menger, F. M.; Bian, J.; Seredyuk, V. A. *Angew. Chem., Int. Ed.* **2004**, *43*, 1265.
(29) Folmer, B. M. *Adv. Colloid Interface Sci.* **2003**, *103*, 99.

(30) Meissner, D.; Grassert, I.; Oehme, G.; Holzhiiter, G.; Vill, V. *Colloid Polym. Sci.* **2000**, *278*, 364.
(31) Rabatic, B. M.; Pralle, M. U.; Tew, G. N.; Stupp, S. I. *Chem. Mater.* **2003**, *15*, 1249.
(32) Kaneka, T.; Nagasawa, H.; Gong, J. P.; Osada, Y. *Macromolecules* **2004**, *37*, 187.
(33) Solomon, O. F.; Cinta, I. J. *J. Appl. Polym. Sci.* **1962**, *6*, 686.
(34) Yusa, S.; Kamachi, M.; Morishima, Y. *Langmuir* **1998**, *14*, 6059.
(35) Bouhamed, H.; Boufi, S.; Magnin, A. *J. Colloid Interface Sci.* **2003**, *261*, 264.
(36) Kalyanasundaram, K.; Thomas, J. K. *J. Am. Chem. Soc.* **1977**, *99*, 2039.
(37) Yekta, A.; Aikawa, M.; Turro, N. J. *Chem. Phys. Lett.* **1979**, *63*, 543.
(38) Tan, J. S.; Gasper, S. P. *Macromolecules* **1973**, *6*, 741.
(39) Yusa, S.; Kamachi, M.; Morishima, Y. *Langmuir* **1999**, *15*, 8826.
(40) Yusa, S.; Kamachi, M.; Morishima, Y. *Macromolecules* **2000**, *33*, 1224.
(41) Chu, D. Y.; Thomas, J. K. *Macromolecules* **1991**, *24*, 2212.
(42) Chen, T. S.; Thomas, J. K. *J. Polym. Sci., Part A: Polym. Chem.* **1979**, *17*, 1103.
(43) Hu, Y.; Smith, G. L.; Richardson, M. F.; McCormick, C. L. *Macromolecules* **1997**, *30*, 3526.
(44) Hu, Y.; Armentront, R. S.; McCormick, C. L. *Macromolecules* **1997**, *30*, 3538.
(45) Kaewsaiha, P.; Matsumoto, K.; Matsuoka, H. *Langmuir* **2005**, *21*, 9938.
(46) Matsuoka, H.; Matsutani, M.; Mouri, E.; Matsumoto, K. *Macromolecules* **2003**, *36*, 5321.
(47) Matsuoka, H.; Maeda, S.; Kaewsasiha, P.; Matsumoto, K. *Langmuir* **2004**, *20*, 7412.
(48) Balomenou, I.; Bokias, G. *Langmuir* **2005**, *21*, 9038.
(49) Rosen, M. J. *Surfactants and Interfacial Phenomena*; John Wiley and Sons: New York, 1978.
(50) Penfold, J.; Tucker, I.; Thomas, R. K.; Taylor, D. J. F.; Zhang, J.; Bell, C. *Langmuir* **2006**, *22*, 8840.

BM061235R